Electrohydrodynamic instabilities of DNA aggregates: a mean field description

2004 J. Phys.: Condens. Matter 16 S3987

(http://iopscience.iop.org/0953-8984/16/38/016)

INSTITUTE OF PHYSICS PUBLISHING JOURNAL OF PHYSICS: CONDENSED MATTER

J. Phys.: Condens. Matter **16** (2004) S3987–S3998 PII: S0953-8984(04)78574-4

Electrohydrodynamic instabilities of DNA aggregates: a mean field description

R Castañeda-Priego[1], H H von Grünberg[1] and M Kollmann[2]

[1] Fachbereich Physik, Universität Konstanz, D-78457, Konstanz, Germany
[2] Fachbereich Physik, Universität Freiburg, D-79104, Freiburg, Germany

Received 26 March 2004
Published 10 September 2004
Online at stacks.iop.org/JPhysCM/16/S3987
doi:10.1088/0953-8984/16/38/016

Abstract

In this work we investigate the experimentally observed electrohydrodynamic instabilities in a confined suspension of lambda-DNA under strong electric fields. We model the underlying stochastic motion of the DNA coils on a coarse grained level, using continuous functions to describe the charge density of the system in space and time. We find, within our approach, that in contrast to previous results there are no long ranged violations of electroneutrality around aggregates of lambda-DNA. We also show that although the corresponding Debye layer is small on the surface of a given aggregate, the electric field can induce a flow field of the solvent which in turn results in a stable pattern of aggregates, which is in agreement with the experimental observations.

1. Introduction

Separation of DNA molecules by size using a capillary electrophoretic mechanism is frequently used in medical applications, such as molecular genetic ones, in order to understand physical, chemical and biological properties of DNA. Under some conditions depending on the polyelectrolyte properties, on the applied electric field, or on the confinement geometry, electrohydrodynamical instabilities in solutions of DNA have been observed and investigated experimentally and theoretically [1].

We are here interested in the experimental study of electrohydrodynamical instabilities carried out by Mitnik *et al* [2]. In this experiment a DNA solution, confined between two glass plates, is exposed to an (AC or DC) external electric field. Figure 1 presents a sketch of the main experimental finding. At $t = 0$ the aggregate possesses a coil configuration. Immediately after the application of the field the aggregate is stretched in a direction perpendicular to the external field. After a few more seconds ($t \geqslant 3$ s), the aggregate finds a metastable configuration with tilted bands showing a zigzag pattern. In a DC field the angle between the bands and the external field was found to be $\pm 45°$; a solvent flow circulating around the aggregate could be

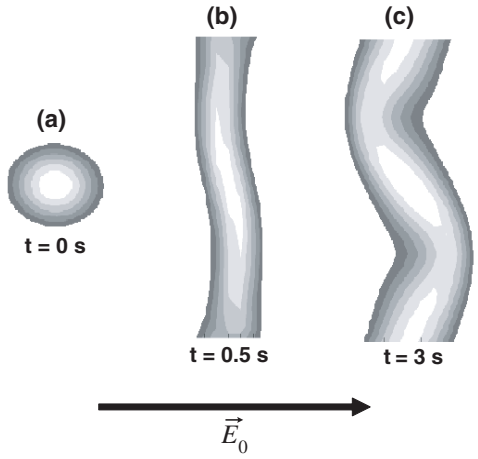

Figure 1. A schematic drawing of the dynamical evolution of a droplet of concentrated DNA solution in an electrolyte under strong electric fields, as observed in the experiments by Mitnik *et al* [2]. The DNA solution is confined between two glass plates and exposed to an (AC or DC) external electric field, $\vec{E}_0$, applied parallel to the plates. The figure shows the top view of the droplet, in a direction perpendicular to the glass plates. (a) $t = 0$, coil configuration. (b) $t = 0.5$ s, stretching of the DNA aggregate in the perpendicular direction of $\vec{E}_0$. (c) $t \geqslant 3$ s, quasi-stationary state: a (metastable) zigzag pattern has formed.

observed. The pattern disappeared at larger times when the diffusion started dominating the dynamics of the DNA aggregate [1, 2].

This interesting behaviour, known also in chaotic systems [3], has also been observed in colloid suspensions [4, 5], in which the interparticle interaction is dominated by strong dipole–dipole interactions, resulting from the large asymmetry of dielectric constants between the solvent and the colloidal material. This dipole–dipole interaction forms the basis of theories of electrorheological fluids [6–8], which when combined with hydrodynamic interactions may explain the experiments in [4]. However, this explanation is certainly not applicable to the system studied by Mitnik *et al*, which is lacking any sort of dipolar interaction. Isambert *et al* [9] suggested a theoretical explanation for the observations of Mitnik *et al* which is essentially based on the electrokinetic equations [10]. These authors argued that a perturbation of the ionic density profiles over large distances (micrometres) led to a local 'breakdown of electroneutrality', which induces a circulating flow field around the DNA aggregates leading to the striking zigzag patterns. In our numerical study, we have found free charges only in a thin (nanometre) double layer close to the surface of the DNA aggregates, but not in regions extending over a micrometre. As regards the key role played by the circulating solvent flow, we come to the same conclusion as Isambert *et al*. We find that the short range charge distribution induces a flow field, which due to the long range nature of the hydrodynamic interactions [11] extends over micrometres, and can ultimately explain the zigzag pattern.

Here, we use a time-dependent mean field approach based on electrokinetic equations, where macroions, coions and counterions are treated at the same level of description. Each ionic species is described by means of a continuous particle density distribution, which satisfies an equation of conservation. The information on the solvent is included in the velocity field, which satisfies a Stokes-like relation. We do not wish to explain here the stretching of the DNA aggregate (figure 1(b)), but rather start from already elongated aggregates and seek for an explanation of why these aggregates are tilted, showing a specific angle with respect to the external field.

Since the early and pioneering work of O'Brien and White [12], the full set of electrokinetic equations have rarely been used to describe dynamical processes. On one hand, this due to the high nonlinearity and complexity of these equations. On the other hand, the large asymmetry in timescales and length scales between the particles in the electrolyte (microions) and the macroions allows one to integrate out the former in the (slow) dynamics of the latter, which gives rise to effective dynamical descriptions [13–15].

The paper is organized as follows. Section 2 presents the electrokinetic equations, and a simple one-dimensional model calculation, performed using input parameters from the experiment of Mitnik *et al*. These results allow us to simplify the electrokinetic equations and to develop a quasi-dynamical perturbative description. In section 3 we apply our theory to simulate the experiment of Mitnik *et al*, resorting to a two-dimensional model system, explaining (i) the circulating flow field around the aggregates, (ii) the rotation of the aggregates and, finally, (iii) the formation of the zigzag pattern.

2. Time-dependent mean field description

2.1. Electrokinetic equations

We study a system that is composed of three charged species, the molecules of DNA and their monovalent coions and counterions. In addition, we have to take account of the solvent which in our case is characterized by a dielectric constant ϵ, a bulk viscosity η and a velocity flow field $\vec{v}$. In a mean field approach, each ionic species can be modelled by a particle number density distribution ρ_i, which in the absence of chemical reactions satisfies the following conservation equation:

$$\partial_t \rho_i(\vec{r};t) + \vec{\nabla}\cdot\vec{J}_i(\vec{r};t) = 0, \tag{1}$$

where $i = 0, +, -$. ρ_0 describes the density profile of the negatively charged DNA molecules and $\rho_{+/-}$ the profiles of the positively and negatively charged ions of the electrolyte. $\vec{J}_i$ is the ionic flux of each ionic species which here is assumed to be composed of three terms:

$$\vec{J}_i(\vec{r};t) = -D_i\vec{\nabla}\rho_i + z_i\mu_i\rho_i\vec{E} + \rho_i\vec{v}, \tag{2}$$

representing contributions arising from Brownian motion, electrophoresis and convection (in that order). Here, D_i are the diffusion coefficients and μ_i the corresponding mobilities. Both quantities are taken to be constant. The quantity z_i takes the value $+1$ (-1) if the charged particle is positive (negative). The aggregate is always assumed to be permeable to the ionic flux. The electric field $\vec{E}$ satisfies the Poisson equation

$$\vec{\nabla}\cdot\vec{E}(\vec{r};t) = \frac{e}{\epsilon}(\rho_+ - \rho_- - \rho_0) \equiv \frac{e}{\epsilon}\rho_{\mathrm{T}}(\vec{r};t), \tag{3}$$

where e is the elementary charge and $\rho_{\mathrm{T}}(\vec{r};t)$ the density of all free charges (total charge distribution).

We assume (the simplest approximation) that the velocity field obeys the Navier–Stokes equation for small Reynold numbers and we also consider the solvent to be an incompressible fluid. Then, the velocity field results from the so-called creeping flow equations [11]

$$\eta\vec{\nabla}^2\vec{v} - \vec{\nabla}P = -\vec{F}, \tag{4}$$

$$\vec{\nabla}\cdot\vec{v} = 0, \tag{5}$$

where P is the pressure in the system and $\vec{F}$ the force acting on each point of the suspension, given here by

$$\vec{F}(\vec{r};t) = e\rho_{\mathrm{T}}(\vec{r};t)\vec{E}(\vec{r};t). \tag{6}$$

The set of equations (1)–(5) is known as the 'electrokinetic equations' [10]. It is solved here numerically to study a DNA solution under a strong DC electric field, $\vec{E}_0$. The whole problem depends on a large number of parameters: $D_i, \mu_i, z_i, c_s, c_0, \epsilon, \eta, \vec{E}_0$. Focusing on a specific experiment, we here fix all these parameters to the values realized in the system of Mitnik *et al* [2]. These are: $D_0 = 10^{-12}$ m^2 s^{-1}, $D \equiv D_+ = D_- = 1000D_0$, $\mu_0 = 3 \times 10^{-8}$ m^2 V^{-1} s^{-1}, $\mu \equiv \mu_+ = \mu_- = 10^{-7}$ m^2 V^{-1} s^{-1}, $z_0 = z_- = -z_+ = -1$, $\epsilon = 10^{-9}$ F m^{-1}, $\eta = 10^{-3}$ Pa s^{-1} and the external field $E_0 = 300$ V cm^{-1}. The concentration of DNA molecules is $c_0 = 10^{-3}$ mol l^{-1}, that of the salt ions, $c_s = 50c_0$. The timescale is set to $\tau \equiv l^2/D$ where $l = 1$ μm is a typical length scale in our problem. It is the timescale connected with the diffusion of the electrolyte ions which is of order 10^{-3} s.

The electrokinetic equations are solved numerically with the appropriate set of initial conditions and periodic boundary conditions on a rectangular lattice with a uniform grid. We use a Crank–Nicholson scheme plus a time splitting operator to discretize and guarantee the stability of the set of equations. Also, we use a two-dimensional standard discrete Fourier transform algorithm with periodic boundary conditions.

2.2. One-dimensional analysis

The driving force in equation (4) is the total charge distribution ρ_T times the electric field. In other words, by identifying the regions in space where $\rho_T \neq 0$ we localize the regions where the force field acts on the fluid of the solvent. Since the concentration of salt ions is a factor 50 higher than that of the DNA charges, ρ_T can be expected to differ from zero only in the small volume of the double layer close to the DNA aggregate.

To set the stage we first study the effect of the high salt concentration on ρ_T; we set the velocity field to zero, $\vec{v} = 0$, and consider the electrokinetic equations in a one-dimensional model derived from the system in an early stage of the zigzag formation (figure 1(b)), and model the shape of the aggregate simply by

$$\frac{\rho_0(x; t = 0)}{c_s} = \begin{cases} \dfrac{c_0}{c_s} = 0.02 & x \leqslant |\Delta/2|, \\ 0 & \text{elsewhere}, \end{cases} \tag{7}$$

where $\Delta = 2$ μm denotes the width of the aggregate (estimated value taken from the experiment [2]). The external field is applied in the positive x direction.

Figures 2(a) and (b) show the coion and counterion profiles at different times. Antisymmetric profiles are found with a depletion of small ions on one side of the aggregate and an excess of salt on the other side. This phenomenon, called concentration polarization, has long been known and has been analysed to understand ionic fluxes through charged membranes [16, 17]. Figure 2(c) compares ρ_+ and ρ_-, and shows that the two profiles are identical on either side of the aggregate. This implies that in the regions where a salt excess/depletion is observed, the system is nevertheless electrically neutral. In contrast to what has been predicted in [9], no 'breakdown of electroneutrality' could be found here. Free charges are found only in the very small volume of the double layer, as can be seen from the total charge distribution $\rho_T = \rho_+ - \rho_- - \rho_0$ plotted in figure 2(d). Due to the high concentration of salt, the thickness of the double layer is only of the order of 10^{-3} μm. We emphasize that figure 2(d) does not show the charge distribution of the equilibrium double layer. Due to the external field E_0, it is not perfectly symmetric, which becomes obvious from figure 2(e) showing the difference between the distribution ρ_T for finite E_0 (figure 2(d)) and for vanishing external field (the equilibrium double layer).

Furthermore, figures 2(a) and (b) demonstrate that the stationary state is reached after a comparatively short time of only $\approx 5\tau$. By contrast, the timescale for the electrophoretic

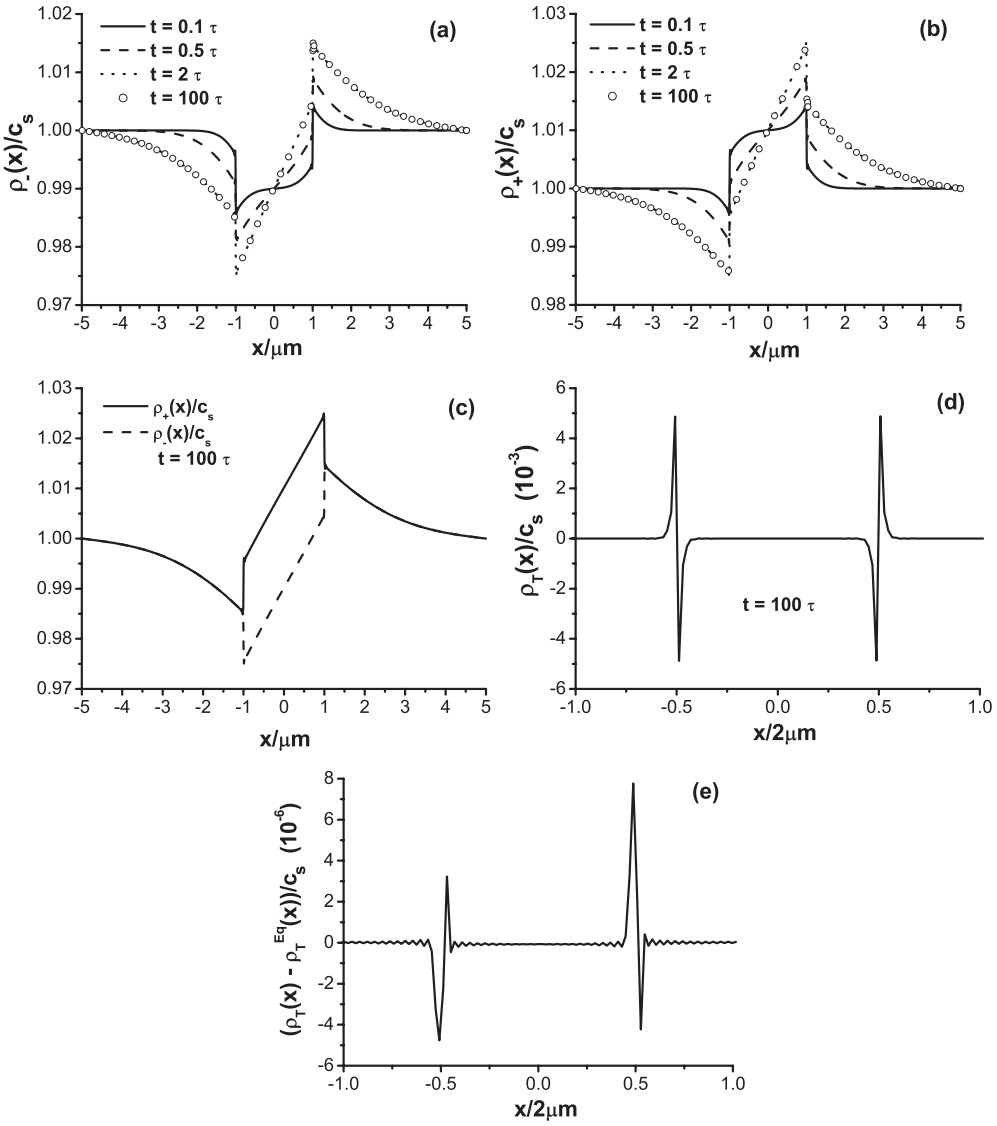

Figure 2. ((a), (b)) Time evolution of coion (a) and counterion (b) density profiles in the neighbourhood of the DNA aggregate, characterized by a one-dimensional rectangle function, equation (7). The aggregate, centred at $x = 0$, has a width of 2 μm. The density is scaled with the reservoir salt concentration c_s. (c) Comparison of the stationary coion and counterion profiles in (a) and (b). (d) The stationary total charge distribution $\rho_T = \rho_+ - \rho_- - \rho_0$, as obtained from the profiles in (a) and (b) and from equation (7). (e) The difference of ρ_T for $E_0 = 300$ V cm^{-1} and for $E_0 = 0$. All input parameters are chosen such as to simulate the experiments of Mitnik *et al* [2].

motion of the aggregate is $\sim 50\tau$, and for its diffusional motion about 1000τ. In other words, the formation of the ion profiles can be considered to be infinitely fast on the timescale of the aggregate which we are interested in. One can check this more explicitly with our one-dimensional model by solving the electrokinetic equation for a moving aggregate (equation (7) with a typical time dependence). Indeed, there is hardly any effect of the motion of the aggregate

on the total charge distribution $\rho_{\mathrm{T}}(\vec{r};t)$. This splitting of timescales is used below to justify the approximation, $\partial_t \rho_{\mathrm{T}} = 0$.

2.3. Quasi-dynamical perturbative description

The solution of the electrokinetic equations in 2D or 3D becomes numerically very demanding. One can considerably simplify the electrokinetic equations by exploiting some of the observations just made. In particular, we focus on the equation of motion for the total charge distribution and its solution, which is one of the key quantities in the creeping flow equations.

The three equations of motion (one for each ionic species; see equation (1)) are interrelated through the total charge distribution, $\rho_{\mathrm{T}}(\vec{r};t)$. First, we linearize the electrolyte distributions around the mean value, $\rho_{+/-} = c_{\mathrm{s}} + \delta\rho_{+/-}$. Figure (2) demonstrates that, indeed, $|\delta\rho_{+/-}| \ll c_{\mathrm{s}}$. The electric field due to the charged species, $\delta\vec{E}$, decays as fast as the total charge distribution, and can be as strong as the external field inside the double layer. However, outside the double layer we may assume that $\vec{E} = \vec{E}_0 + \delta\vec{E}$, where $\delta E \ll E_0$, which is valid at large length scales. Ignoring second-order terms, i.e., $\delta\rho_{+/-}\delta\vec{E} \simeq 0$, we then find, after some algebra,

$$\begin{aligned}\partial_t\rho_{\mathrm{T}} - D\vec{\nabla}^2\rho_{\mathrm{T}} + \mu\vec{E}_0\cdot\vec{\nabla}\rho_{\mathrm{T}} + \vec{v}\cdot\vec{\nabla}\rho_{\mathrm{T}} + \frac{2\mu c_{\mathrm{s}} e}{\epsilon}\rho_{\mathrm{T}} \\ = D^{\mathrm{eff}}\vec{\nabla}^2\rho_0 - \mu^{\mathrm{eff}}\vec{E}_0\cdot\vec{\nabla}\rho_0 - 2\mu\vec{E}_0\cdot\vec{\nabla}\delta\rho_-,\end{aligned} \tag{8}$$

which is the equation of motion of the total charge distribution. $D^{\mathrm{eff}} \equiv D - D_0 \simeq D$ and $\mu^{\mathrm{eff}} \equiv \mu + \mu_0 \simeq 2\mu$. We next use the fact that the dynamics of the electrolyte ions is much faster than that of the aggregate (figure 2), and set $\partial_t\rho_{\mathrm{T}} = 0$. This assumption holds on the timescale characteristic of the aggregate. Then, equation (8) can be solved in Fourier space:

$$\rho_{\mathrm{T}}(\vec{q}) = -\frac{(D^{\mathrm{eff}}q^2 - \mathrm{i}\mu^{\mathrm{eff}}\vec{E}_0\cdot\vec{q})(Dq^2 + \mathrm{i}\mu\vec{E}_0\cdot\vec{q} - \mathrm{i}\vec{v}\cdot\vec{q})}{(Dq^2 - \mathrm{i}\mu\vec{E}_0\cdot\vec{q} - \mathrm{i}\vec{v}\cdot\vec{q})(Dq^2 + \mathrm{i}\mu\vec{E}_0\cdot\vec{q} - \mathrm{i}\vec{v}\cdot\vec{q}) + \frac{2\mu c_{\mathrm{s}}e}{\epsilon}(Dq^2 - \mathrm{i}\vec{v}\cdot\vec{q})}\rho_0(\vec{q}), \tag{9}$$

where, for the moment, we have considered a constant velocity field $\vec{v}$. The effect of the approximations made in deriving equation (9) can be tested by reproducing ρ_{T} in figure 2(d), with $\vec{v} = 0$. The resulting curve is almost indistinguishable from the curve in figure 2(d), which is due to the fact that the assumption $\delta E \ll E_0$ fails only in a negligibly small region of the double layer. So, ρ_{T} resulting from equation (9) seems to be an excellent approximation everywhere in space, even inside the double layer. For the one-dimensional case, the inverse Fourier transform of $\rho_{\mathrm{T}}(\vec{q})$ in equation (9) can be calculated analytically. In two and three dimensions this is not possible; the inverse transformation has to be carried out numerically.

We next exploit the specific geometry of the experiment we here wish to describe [2]. The glass plates are separated by a distance $d \simeq 10\ \mu$m. The DNA aggregates remain on the mid-plane between the two plates, i.e., the movement in the perpendicular direction to the plates is considerably suppressed and can be ignored. This allows us to focus our investigation just on the mid-plane and to apply another set of approximations. We here follow [9]. We assume that the velocity field between the plates is well described by a parabolic profile, having the following form [18]:

$$\vec{v}(\vec{r}) = \left[1 - (2z/d)^2\right]\vec{v}_{2\mathrm{D}}(x,y), \tag{10}$$

where $\vec{v}_{2\mathrm{D}}$ represents the velocity field on a x–y plane parallel to the plates. Equation (10) is placed into equations (4) and (5) at $z = 0$ (mid-plane), where the parabolic profile reaches its maximum value. Also, we apply the well-known Hele–Shaw approximation which consists

in assuming $-\vec{\nabla}P + \vec{F}$ in equation (4) to be independent of the z component. Then, the two-dimensional version of the creeping flow equations reads

$$\eta\left(\vec{\nabla}_{2\mathrm{D}}^2 - 8/d^2\right)\cdot\vec{v}_{2\mathrm{D}} - \vec{\nabla}P = -\vec{F}, \tag{11}$$

$$\vec{\nabla}_{2\mathrm{D}}\cdot\vec{v}_{2\mathrm{D}} = 0. \tag{12}$$

Due to the linearity of the creeping flow equations they can be rewritten as

$$\vec{v}_{2\mathrm{D}}(\vec{q}) = \underline{\underline{T}}(\vec{q})\cdot\vec{F}(\vec{q}), \tag{13}$$

where $\vec{F}(\vec{q})$ is the Fourier transform of the equation (6) and $\underline{\underline{T}}(\vec{q})$ is the two-dimensional Oseen tensor [11], which has the form

$$\underline{\underline{T}}(\vec{q}) = \frac{1}{\eta\left(8/d^2 + q^2\right)}\left[\hat{1} - \frac{\vec{q}\vec{q}}{q^2}\right], \tag{14}$$

where $\hat{1}$ is the 2×2 identity matrix and $\vec{q}\vec{q}$ denotes a dyadic product. The Poisson equation, equation (3), can also be solved in Fourier space. Then, each component of the electric field is given by

$$\delta E_k(\vec{q}) = -\mathrm{i}\frac{e}{\epsilon}\frac{q_k}{q^2}\rho_{\mathrm{T}}(\vec{q}), \tag{15}$$

where $k = x, y$. The last equation describes the time evolution of the DNA aggregate; it results from the combination of equations (1), (2) and (5) for the component $i = 0$:

$$\partial_t\rho_0 - D_0\vec{\nabla}^2\rho_0 - \mu_0\vec{\nabla}\cdot(\rho_0\vec{E}) + \vec{v}\cdot\vec{\nabla}\rho_0 = 0. \tag{16}$$

We are now in a position to describe our numerical scheme. The four central equations are (i) equation (9), providing a solution for ρ_{T}, (ii) Poisson's equation in equation (15), (iii) equation (13), the creeping flow equation, and (iv) equation (16) for the aggregate dynamics. They are solved iteratively and always with periodic boundary conditions. We start with a given model form of $\rho_0(\vec{r};\, t = 0)$ and, assuming $\vec{v}$ to be zero everywhere, calculate $\rho_{\mathrm{T}}(\vec{q})$ from equation (9) and place this into the Poisson equation (15) to obtain $\vec{E}(\vec{q})$. Both $\vec{E}(\vec{q})$ and $\rho_{\mathrm{T}}(\vec{q})$ are needed in equation (13) to compute the Fourier transform of the velocity field. We then compute the spatial average of the velocity field and place this in equation (9) to compute again $\rho_{\mathrm{T}}(\vec{q})$. This cycle is iterated until convergence is achieved. The velocity field and the electric field, after a transformation back to real space, are finally used in equation (16) to propagate the aggregate ρ_0 by one time step.

From the numerical point of view, this procedure means a considerable simplification. Instead of the large set of nonlinear differential equations, the electrokinetic equations, one now has to solve just one differential equation, equation (16), and the Fourier inverse of the equations (9), (13) and (15). One should keep in mind, however, that our description is adapted to a specific experiment and is valid only in the high salt limit and if strong external electric fields are applied.

We would like to point out that our quasi-dynamical description for the total charge distribution given in equation (9) reduces to that proposed by Isambert *et al* [9] on ignoring the diffusion effects and velocity fields in equation (9) and assuming that the system has reached the stationary state, $\partial_t\rho_{\mathrm{T}} = 0$. In that case, the total charge distribution is given by three terms which depend on the electrophoretic and diffusional properties of the aggregate and the gradient of the salt concentration. This last term was already used in the Isambert *et al* approach in order to calculate the velocity and electric fields in a similar way to in equations (13) and (15), respectively. However, such a procedure is not fully self-consistent and could give rise to unphysical effects such as the 'breakdown of the local electroneutrality' at large distances as addressed in [9].

3. Two-dimensional simulation of the experiment

3.1. Circulating velocity flux

We first model the charge distribution of a lambda-DNA aggregate by a two-dimensional rectangular function

$$\frac{\rho_0(x, y)}{c_s} = \begin{cases} 0.02 & x \leqslant |\Delta/2| \text{ and } y \leqslant |L/2|, \\ 0 & \text{elsewhere,} \end{cases} \tag{17}$$

where L (=2 μm) is the length of the aggregate, which is larger than its width Δ (taken here to be 1 μm). In the strong electric field limit, $E_0 \gg \delta E$, the velocity field, given by equation (13), reduces to

$$\vec{v}_{2D}(\vec{q}) = \frac{e\rho_T(\vec{q})}{\eta\left(8/d^2 + q^2\right)}\left[\vec{E}_0 - \frac{\vec{q}\cdot\vec{E}_0}{q^2}\vec{q}\right]. \tag{18}$$

Equation (18) illustrates that the flow field depends explicitly on the direction of the external field. For the case at hand, using the initial aggregate configuration described by equation (17), we found that the maximum velocity amplitude ($v_{2D} \simeq 10\ \mu\text{m s}^{-1}$) predicted by equation (18) is in quantitative agreement with the experiments [2].

To explore the system we first study the evolution of the velocity field for the model aggregate in equation (17) which, for the moment, is not allowed to move in space. The external electric field forms an angle $\theta = 45°$ with respect to the x-axis; that is, we have finite values for the components $E_{0,x}$ and $E_{0,y}$. Figure 3(a) shows a cut in the x direction of the velocity field at $y = L/2$. The strong peaks are important; the oscillations are artefacts due to numerical noise. Comparison with figure 2(d) shows that the velocity distribution closely follows the total charge distribution. The field couples to the positive and negative charges of the double layer and drags them in opposite directions; this can be observed on both sides of the aggregate. It is clear that if the electric field is perpendicular to the aggregate, i.e., if $E_{0,y} = 0$, the velocity field is zero at $y = L/2$. Like the total charge distribution in figure 2(d), the peak structure in figure 3(a) is not symmetric, as becomes evident when adding the two peaks. This is plotted in figure 3(b). One may consider this flow field as the net velocity field resulting from a coarse graining procedure. It is seen to be in the positive y direction on one side and in the negative y direction on the other side. Clearly, this net flux results from the asymmetry in the total charge distribution which in turn is due to the presence of an external field. It is then clear that the net flux is zero if $E_{0,x} = 0$. At this point, one recognizes the twofold role of the electric field: it is necessary

(i) to polarize the double layer for an asymmetric charge distribution on the right- and the left-hand sides of the aggregate, and
(ii) to drag the charges through the solvent, within both layers of the double layer and parallel to the surface of the aggregate.

This requires finite values of both the components $E_{0,x}$ and $E_{0,y}$, that is, a finite angle θ between the director of the aggregate and the electric field. Of course, the same argument is valid at the top and bottom of the aggregate. This means that an asymmetric double layer is observed due to $E_{0,y} \neq 0$, and a net flux resulting from the coupling between the free charges in those regions with a finite $E_{0,x}$.

The whole (coarse grained) velocity distribution in the x–y plane is to be seen in the inset figure. It is a clockwise circulating flux, confined essentially to the region occupied by the double layer. In agreement with the explanation given above, the flux should be anticlockwise

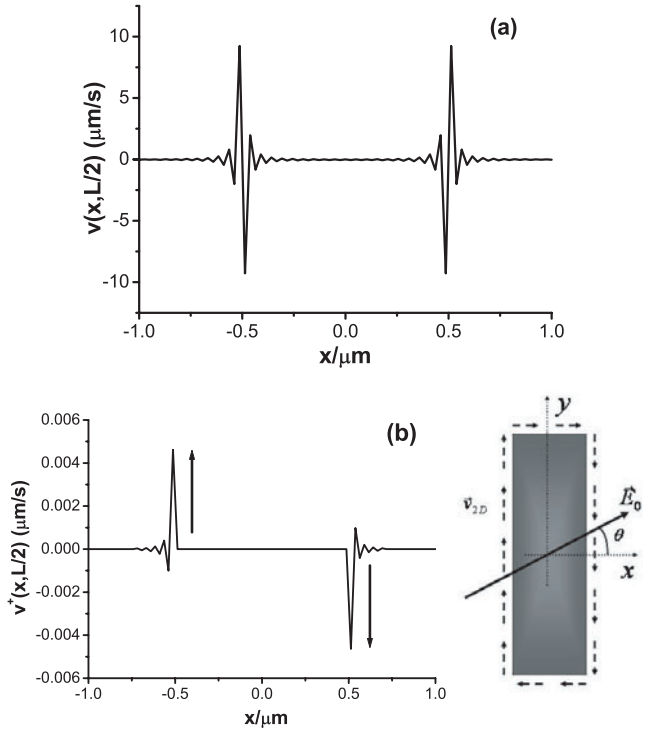

Figure 3. (a) A cut through the solvent flow field at $y = L/2$ in the strong electric field limit around the surface of a two-dimensional aggregate, modelled here by a rectangular function of width 1 μm in the x direction and of length 2 μm in y direction which is centred on the origin of the coordinate system. (b) The coarse grained velocity field, obtained from (a) by adding the two peaks on either side of the aggregate. The inset shows the net velocity field in two dimensions.

if the angle between the external field and the aggregate is negative. We have explicitly checked that this is the case. A circulating velocity field has also been observed experimentally [2, 9].

3.2. Rotating aggregate and zigzag pattern formation

We now study the dynamics of the aggregate. We wish to show that the circulating velocity field produced by the asymmetry of the total charge distribution will lead to a rotation of the aggregate towards a quasi-stationary position where the shear stress is extremal. We use an aggregate model that is numerically more convenient than the rectangular function used so far. In the following, the aggregate is represented by a ellipsoidal Gaussian function with two half-axes between 1 and 2 μm in length; see inset of figure 4. The direction of the aggregate is specified by an orientational vector $\vec{n}$, which initially forms an angle φ_0 with the external field. The angle between $\vec{n}$ and the x-axis is defined by α. Explicitly, the ellipsoidal-like aggregate has the form

$$\frac{\rho_0(x, y)}{c_s} = 0.02 \exp[-(1/a)(x\cos\alpha + y\sin\alpha)^2 + (1/b)(-x\sin\alpha + y\cos\alpha)^2], \tag{19}$$

where the parameters a and b allow us to handle the eccentricity of the aggregate.

The dynamical evolution of the aggregate results from the solution of equation (16). We solve this equation relative to the centre of mass of the aggregate. The evolution of the angular

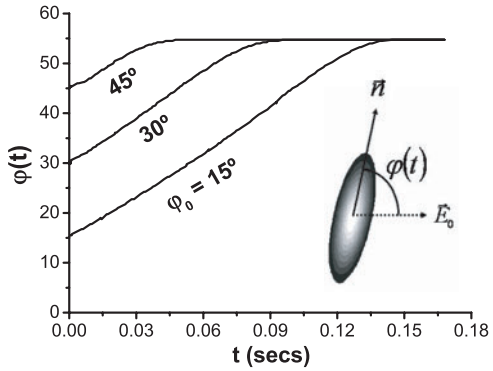

Figure 4. The time evolution of the angular shift of an isolated aggregate having an initial orientation relative to the external electric field of $\varphi_0 = 15°, 30°, 45°$. The aggregate reaches a quasi-stationary state when $\varphi \simeq 55°$.

shift can then be obtained from

$$\Delta\varphi(t) = \frac{\int \rho_0(\vec{r};t)|\vec{r}\times\vec{v}_{2D}|\,d\vec{r}}{\int r^2\rho_0(\vec{r};t)\,d\vec{r}}\Delta t, \tag{20}$$

where $\vec{r} = x\hat{i} + y\hat{j}$ and Δt denotes the time step used in our numerical solution.

Figure 4 shows the angular evolution of the aggregate model for different values of φ_0. The aggregate reaches a quasi-stationary configuration at $\varphi \simeq 55°$ which is independent of the initial values of φ_0. We checked that this result is independent of the box size, the mesh size and the time step used in our numerical scheme. The stable configuration corresponds to the situation with maximum shear velocity. This can be seen by taking $q \to 0$ in the expression of the total charge distribution, equation (4),

$$\rho_T \to -\frac{\mu^{\text{eff}}}{\mu}\rho_0, \tag{21}$$

from which one obtains the following shear velocity:

$$\vec{v}_{2D} = -\frac{c_s d^2}{8\eta}\frac{\mu^{\text{eff}}E_0\rho_0}{\mu}\vec{n}_M, \tag{22}$$

with $\vec{n}_M = (\cos(\theta)\cos(\varphi) - \sin(\theta)\sin(\varphi))\hat{i} + (\cos(\theta)\sin(\varphi) + \sin(\theta)\cos(\varphi))\hat{j}$. θ is the angle between $\vec{E}_0$ and the x-axis, φ that between $\vec{E}_0$ and $\vec{n}$. From this equation we can easily check that the shear velocity reaches a maximum value, independent of θ, when $\varphi = 60°$, which is in a qualitative agreement with the value observed in figure 4.

We next study the angular evolution of a collection of ellipsoidal aggregates. Specifically, we analyse the dynamical behaviour of the system depicted in figure 5. Each aggregate is characterized by an orientational vector $\vec{n}_i$ ($i = 1, 2, 3, 4$). We here allow for just one degree of freedom given by the angle φ between neighbouring aggregates as indicated in the figure. Together with the periodic boundary conditions which we have applied here, this simulates a macroscopic sample of DNA aggregates forming zigzag patterns, as observed in the quoted experiment.

In figure 5 we show the angular shift as a function of time for five different values of the initial angle φ_0. In all cases, the quasi-stationary configuration is reached when the angle of tilt is $\varphi \simeq 45°$, which is in excellent agreement with the experimental observation [2]. We find a solvent flow circulating clockwise (anticlockwise) around the aggregates $\vec{n}_1$ and $\vec{n}_4$

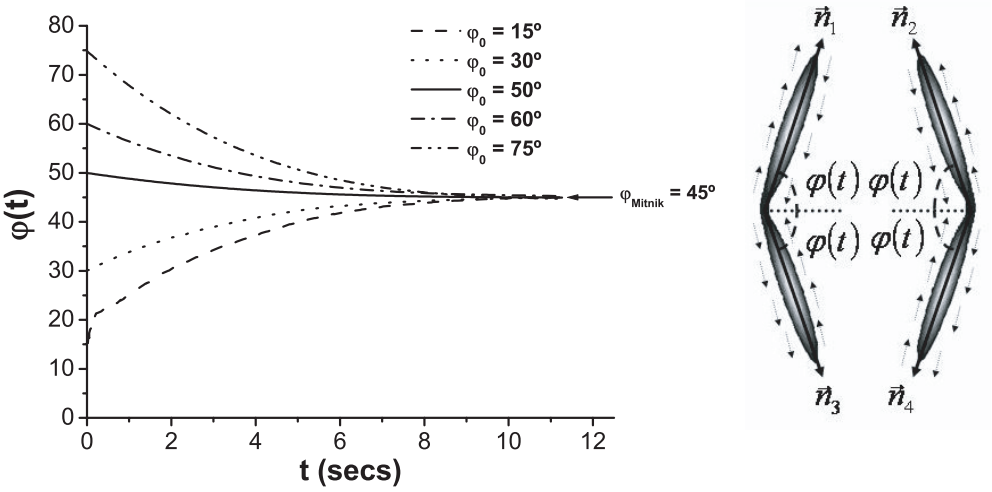

Figure 5. The time evolution of the angular shift of a collection of four DNA model aggregates, starting from various initial angles φ_0 as indicated. Due to hydrodynamic interactions the aggregates now find a quasi-stationary state when $\varphi \simeq 45°$.

$(\vec{n}_2, \vec{n}_3)$. The collection of aggregates tries to find a spatial arrangement such as to minimize the friction between the circulating flow fields around each aggregate. This is obviously the case if $\varphi \simeq \pm 45°$. It is thus recognized that the circulating velocity field is not to be seen as a side-effect, but rather as the origin of the formation of the zigzag pattern. The 10° difference in quasi-stationary state angle found between aggregates in isolation (figure 4) and ones gathered in a group (figure 5), highlights the important role played by the hydrodynamical interactions.

4. Conclusions

In the present paper we have focused on one class of instabilities observed in experiments performed by Mitnik *et al* [2]. We have used a time-dependent mean field description, based on the electrokinetic equations, in order to understand the main mechanism responsible for the tilted bands and the formation of zigzag patterns in DNA solutions under the influence of a strong electric fields. Reducing the full set of electrokinetic equations, we developed and tested a self-consistent, quasi-dynamical and much simpler description which is valid for high salt concentrations and strong electric fields.

Based on our numerical studies presented in this paper, we suggest the following explanation for the formation of tilted bands.

(i) Due to the high salt content, free charges can be found only in the thin $\mathcal{O}(10^{-3}\ \mu\text{m})$ double layer close to the surface of the aggregate. This double layer is asymmetric if the electric field has a component perpendicular to the double layer.

(ii) The driving force in the creeping flow equation is the charge distribution times the electric field. For this reason, the flow field is essentially confined to a small region near to the surface of the aggregates where free charges are to be found. If the double layer is asymmetric, there are net flows in opposite directions on either side of the aggregate, and, as a result of this, one finds a circulating flow around the aggregate. This requires an electric field component parallel to the electric double layer. The electric field is thus

necessary to polarize the double layer, but also to drag the charges within the double layer, i.e., parallel to the double layer. In other words, a circulating flow is possible only for angles φ between the electric field and the aggregate direction that are between zero and 90°.

(iii) An isolated aggregate reaches a quasi-stationary state at 55° where the flow field is found to be extremal.

(iv) By contrast, a collection of aggregates forms tilted bands with a relative stationary state angle of 45°. This diamond-like arrangement of aggregates, also found in the experiment of Mitnik *et al*, seems to result from hydrodynamical interactions that can be associated with the solvent circulation around the individual aggregates.

Acknowledgments

This work was supported by the Transregio SFB 6018. We would like to thank to Professors R Klein and M Fuchs for stimulating and helpful discussions.

References

[1] Viovy J L 2000 *Rev. Mod. Phys.* **72** 813
[2] Mitnik L, Heller C, Prost J and Viovy J L 1995 *Science* **267** 219
[3] Cross M C and Hohenberg P C 1993 *Rev. Mod. Phys.* **65** 851
[4] Hu Y, Glass J L, Griffith A E and Fraden S 1994 *J. Chem. Phys.* **100** 4674
[5] Dzubiella J and Löwen H 2002 *J. Phys.: Condens. Matter* **14** 9383
[6] Halsey T C and Toor W 1990 *Phys. Rev. Lett.* **65** 2820
[7] Klingenberg D J and Zukoski C F IV 1989 *Langmuir* **6** 15
[8] Martin J E, Odinek J, Halsey T C and Kamien R 1998 *Phys. Rev.* E **57** 756
[9] Isambert H, Ajdari A, Viovy J L and Prost J 1997 *Phys. Rev.* E **56** 5688
[10] Hunter R 1989 *Foundations of Colloid Science* vol 2 (Oxford: Oxford University Press)
[11] Dhont J K G 1996 *An Introduction to Dynamics of Colloids* (Amsterdam: Elsevier)
[12] O'Brien R W and White L R 1978 *J. Chem. Soc. Faraday Trans.* 2 **74** 1607
[13] Medina-Noyola M 1988 *Phys. Rev. Lett.* **60** 2705
[14] Nägele G 1996 *Phys. Rep.* **272** 215
[15] Méndez-Alcaraz J M and Alarcón-Waess O 2003 *Developments in Mathematical and Experimental Physics* (*Statistical Physics and Beyond* vol B) (Dordrecht: Kluwer–Academic) p 45
[16] Rubinstein I and Shtilman L 1979 *J. Chem. Soc. Faraday Trans.* 2 **75** 281
[17] Rubinstein I 1981 *J. Chem. Soc. Faraday Trans.* 2 **77** 1595
[18] Guyon E, Hulin J P, Petit L and Mitescu C D 2001 *Physical Hydrodynamics* (Oxford: Oxford University Press)